

## Potent and Orally Active Small-Molecule Inhibitors of the MDM2–p53 Interaction

Shanghai Yu,<sup>†,§</sup> Dongguang Qin,<sup>†,§</sup> Sanjeev Shangary,<sup>†</sup>  
 Jianyong Chen,<sup>†</sup> Guoping Wang,<sup>†</sup> Ke Ding,<sup>†</sup>  
 Donna McEachern,<sup>†</sup> Su Qiu,<sup>†</sup> Zaneta Nikolovska-Coleska,<sup>†</sup>  
 Rebecca Miller,<sup>†</sup> Sanmao Kang,<sup>‡</sup> Dajun Yang,<sup>‡</sup> and  
 Shaomeng Wang<sup>\*,†</sup>

<sup>†</sup>Comprehensive Cancer Center and Departments of Internal Medicine, Pharmacology, and Medicinal Chemistry, University of Michigan, 1500 E. Medical Center Drive, Ann Arbor, Michigan 48109, and <sup>‡</sup>Ascenta Therapeutics Inc., 101 Lindenwood Drive, Malvern, Pennsylvania 19355. <sup>§</sup>Equal contributions.

Received September 20, 2009

**Abstract:** We report herein the design of potent and orally active small-molecule inhibitors of the MDM2–p53 interaction. Compound **5** binds to MDM2 with a  $K_i$  of 0.6 nM, activates p53 at concentrations as low as 40 nM, and potently and selectively inhibits cell growth in tumor cells with wild-type p53 over tumor cells with mutated/deleted p53. Compound **5** has a good oral bioavailability and effectively inhibits tumor growth in the SJSA-1 xenograft model.

The p53 tumor suppressor is an attractive cancer therapeutic target because its tumor suppressor activity can be stimulated to eradicate tumor cells.<sup>1–3</sup> In tumor cells with wild-type p53, the p53 activity is effectively inhibited by its endogenous inhibitor, the human MDM2 protein, through direct binding to p53.<sup>4,5</sup> The interaction site between MDM2 and p53 proteins is mediated by a well-defined pocket in MDM2 and a short helix from p53, making this site attractive for the design of small-molecule inhibitors to block the MDM2–p53 protein–protein interaction.<sup>6,7</sup> Reactivation of p53 by blocking the MDM2–p53 interaction using a small-molecule inhibitor is being pursued as an exciting, new cancer therapeutic strategy.<sup>8–22</sup>

We have recently reported the design of spirooxindoles as a new class of potent, selective, cell permeable, nonpeptidic, small-molecule inhibitors of the MDM2–p53 interaction.<sup>9–11</sup> Using a structure-based approach, we have obtained **1** (MI-63, Figure 1) as a potent and cell-permeable MDM2 inhibitor. Compound **1** binds to MDM2 protein with a low nanomolar affinity in our fluorescence-polarization (FP) based, competitive, biochemical binding assay.<sup>10</sup> Consistent with its mode of action, **1** potently inhibits cell growth in cancer cells with wild-type p53 and is selective over cancer cells with mutated/deleted p53. In our subsequent pharmacokinetic (PK) evaluations, **1** was found to have a poor PK profile and a modest oral bioavailability (Table 2). Hence, **1** is not a suitable candidate for drug development.

Herein, we report our design, synthesis, and evaluation of new analogues of **1** with a goal to discover potent MDM2 inhibitors with improved oral bioavailability and overall PK parameters. Our efforts yielded new, potent small-molecule

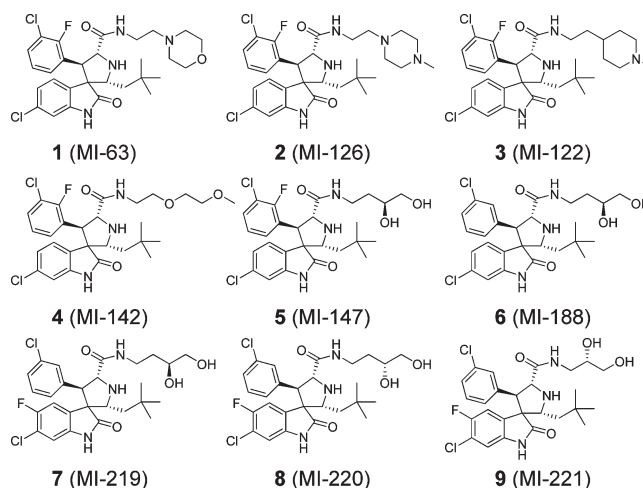


**Figure 1.** Chemical structures of potent MDM2 inhibitors.

**Table 1.** Binding Affinities of MDM2 Inhibitors to MDM2 and Their Activity in Cancer Cell Lines with Wild-Type p53 Status and Selectivity in Cancer Cell Lines with p53 Deletion

compd	binding affinity to MDM2		IC <sub>50</sub> (μM) in cell growth inhibition assay		
	IC <sub>50</sub> ± SD (nM)	K <sub>i</sub> ± SD (nM)	SJSA-1 (p53 WT)	Saos-2 (p53 deleted)	cellular selectivity (SJSA-1/Saos-2)
<b>1</b>	28.3 ± 5.5	1.7 ± 0.5	0.5 ± 0.1	14.1 ± 1.3	28
<b>2</b>	25.7 ± 4.3	1.5 ± 0.4	0.3 ± 0.0	4.6 ± 0.7	15
<b>3</b>	32.4 ± 6.0	2.0 ± 0.5	0.3 ± 0.0	3.3 ± 0.3	11
<b>4</b>	32.4 ± 6.0	0.8 ± 0.3	0.7 ± 0.2	14.2 ± 3.4	20
<b>5</b>	16.4 ± 0.3	0.6 ± 0.1	0.2 ± 0.0	18.2 ± 0.8	91
<b>6</b>	56.0 ± 4.7	4.0 ± 0.4	0.6 ± 0.2	28.8 ± 4.7	48
<b>7</b>	162 ± 75	13.1 ± 6.4	0.7 ± 0.1	15.4 ± 0.8	22
<b>8</b>	157 ± 13	12.6 ± 1.1	1.7 ± 0.1	40.5 ± 3.8	24
<b>9</b>	189 ± 56	15.4 ± 4.8	1.0 ± 0.2	17.8 ± 1.4	18

inhibitors of the MDM2–p53 interaction with excellent oral bioavailability.

Analysis of the predicted binding model for **1** showed that the morpholinyl group is partially exposed to solvent.<sup>10</sup> This suggested that the morpholinyl group in **1** may be replaced by other groups without a detrimental effect on binding to MDM2 and cellular activity. We have therefore carried out chemical modifications of this region to investigate the structure–activity relationship on binding, cellular activity, and PK parameters.

We first designed and synthesized **2** and **3** (Figure 1), in which the morpholinyl group in **1** is replaced by a methylpiperazinyl group or a methylpiperidinyl group, respectively. Our binding experiments showed that these two compounds bind to MDM2 with  $K_i$  of 1.5 and 2.0 nM, respectively (Table 1). Consistent with their high binding affinities to MDM2, they potently inhibit cell growth in the cancer cell lines with wild-type p53 and display excellent selectivity over cancer cell lines with deleted p53 (Table 1 and Supporting Information). However, PK testing showed that while **2** and **3** have an improved PK profile over **1**, the  $c_{max}$  and AUC values are still relatively low with oral dosing (Table 2).

\*To whom correspondence should be addressed. Phone: 734-615-0362. Fax: 734-647-9647. E-mail: shaomeng@umich.edu.

**Table 2.** PK Parameters of MDM2 Inhibitors in Rats with Oral Dosing<sup>a</sup>

compd	oral dose (mg/kg)	$C_{\max}$ (ng/mL)	AUC (0–t) (h· $\mu$ g/L)	$T_{1/2}$ (h)	$F$ (%)
<b>1</b>	25	248 ± 176	321 ± 154	1.3 ± 0.2	10
<b>2</b>	25	274 ± 82	1888 ± 515	3.8 ± 0.5	31
<b>3</b>	25	120 ± 112	1078 ± 891	7.1 ± 1.8	14
<b>4</b>	25	97 ± 28	145 ± 30	1.2 ± 0.2	5
<b>5</b>	50	1514 ± 905	8769 ± 5178	3.9 ± 1.6	21
<b>6</b>	50	805 ± 158	4110 ± 1872	3.0 ± 0.4	19
<b>7</b>	25	3751 ± 1068	7677 ± 328	1.4 ± 0.1	65
<b>8</b>	25	3548 ± 934	11746 ± 2337	3.4 ± 0.5	31
<b>9</b>	25	2067 ± 467	5094 ± 1533	3.2 ± 2.8	18

<sup>a</sup>  $C_{\max}$ : maximum concentration of the compound detected in plasma. AUC: area under the curve.  $T_{1/2}$ : terminal half-life.  $F$ : oral bioavailability.

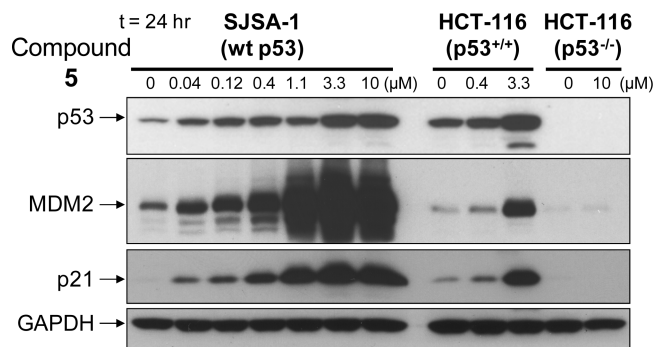
In **1**, **2**, and **3**, the morpholinyl group, the methylpiperazinyl group, and the methylpiperidinyl group are protonated and positively charged at physiological conditions. We hypothesized that these charged groups may contribute to the low  $c_{\max}$  and AUC values with oral dosing for these compounds. We therefore designed **4** and **5** to test if replacement of a positively charged group with a neutral group can improve the oral bioavailability without compromising binding affinity to MDM2 and cellular activity.

Compounds **4** and **5** have  $K_i$  of 0.8 and 0.6 nM to MDM2 protein in our binding assay (Table 1). Both compounds also potentially inhibit cancer cell growth in cancer cell lines with wild-type p53 and display good selectivity over cancer cell lines with deleted p53 (Table 1 and Supporting Information). For example, **5** achieves an  $IC_{50}$  of 0.2  $\mu$ M in inhibition of cell growth in the SJSA-1 osteosarcoma cell line with wild-type p53 and displays a selectivity of 91 times over Saos-2 osteosarcoma cell line with deleted p53 in the same assay (Table 1).

Despite their similar potencies in binding and cellular assays, **4** and **5** have very different PK profiles with oral dosing. Compound **4** with a 1-ethoxy-2-methoxyethyl tail has a very poor PK profile, as indicated by its low AUC and  $c_{\max}$  values. In contrast, **5** with a butyl-1,2-diol tail has a significantly improved PK profile over **1**, **2**, and **3**. Its  $c_{\max}$  at 50 mg/kg oral dosing reaches 1514 ng/mL, and it has an AUC of 8769 h·mg/L. We did not evaluate **5** at 25 mg/kg oral dosage, thereby preventing us from direct comparison of the improvement over **1**. However, if we assume a dose-linearity for the PK parameters of **5**, its  $c_{\max}$  and AUC have improved by 3 and 10 times, respectively, over **1**.

Using **5** as the new lead compound, we next designed and synthesized **6** to evaluate the effect of the 2-F substitution in the phenyl ring on in vitro activity and PK parameters. While **6** still potently binds to MDM2, it is 7 times less potent than **5** (Table 1). Consistent with its weaker binding affinity to MDM2, **6** is 2–3 times less potent than **5** in cell growth inhibition in the SJSA-1 and HCT-116 cell lines with wild-type p53 (Table 1 and Supporting Information). PK evaluations showed that AUC and  $c_{\max}$  for **6** are 2 times lower than those for **5**. Hence, we conclude that the 2-F substitution in the phenyl ring makes a positive impact on binding, cellular activity, and PK parameters in **5**.

We next designed **7** based on the chemical structure of **6** to examine the effect of a 4-F substitution in the oxindole ring on binding, cellular activity, and PK parameters. In direct comparison, **7** is 4 times less potent than **6** in its binding to MDM2. Interestingly, **7** is only slightly less potent than **6** in inhibition

**Figure 2.** Dose-dependent p53 activation induced by **5** in SJSA-1 and HCT-116 cell lines and its specificity in HCT-116 isogenic p53 knockout cell line.

of cell growth in the SJSA-1 and HCT-116 cell lines with wild-type p53 (Table 1 and Supporting Information). Compound **7**, however, has a much improved PK profile with oral dosing over **6**. Compound **7** at 25 mg/kg oral dosing achieves a  $c_{\max}$  of 3751 ng/mL (6.4  $\mu$ M), AUC of 7677 h·mg/L, and an oral bioavailability of 65%.

Using **7** as the template, we performed additional modifications on the butyl-1,2-diol tail to further explore the structure–activity relationship at this site on binding, cellular activity, and PK parameters. Change of the chiral center in the tail from the *S*-configuration to *R*-configuration leads to **8**. Compound **8** has the same binding affinity to MDM2 as **7** but is slightly less potent than **7** in cell growth inhibition in the SJSA-1 and HCT-116 cell lines (Table 1 and Supporting Information). Compounds **7** and **8** also have very similar PK profiles in terms of their  $c_{\max}$  and AUC values at 25 mg/kg oral dosing. These data indicate that the chirality does not have a significant impact on the binding affinity to MDM2, cellular activity, and PK parameters.

We next examined the effect of shortening the tail from butyl-1,2-diol to propyl-1,2-diol, which leads to **9**. Compound **9** is as potent as **7** and **8** in binding to MDM2 and in cell growth inhibition in SJSA-1 and HCT-116 cancer cell lines with wild-type p53 (Table 1 and Supporting Information). Our PK studies, however, showed that **9** is slightly inferior to **7** and **8** in terms of  $c_{\max}$  and AUC values.

We tested **5** for its ability to activate p53 in cancer cells by Western blot analysis (Figure 2). Compound **5** effectively and dose-dependently activates p53 in the SJSA-1 cancer cell line with wild-type p53 and overexpressed MDM2 at concentrations as low as 40 nM, as evident by the robust increase of p53 protein, as well as the MDM2 and p21 proteins, two p53 targeted gene products. Compound **5** also activates p53 and induces an increase of MDM2 and p21 proteins in the HCT-116 cancer cell line with wild-type p53 in a dose-dependent manner but not in the isogenic HCT-116 cell line with deleted p53 (Figure 2).

We next compared **5**, **7**, and racemic nutlin-3 for their ability to activate p53 in the SJSA-1 cell line (Figure 3A). Both **5** and **7** effectively and dose-dependently activate p53 in the SJSA-1 cancer cell lines with wild-type p53, evident by robust increase of p53 protein, as well as MDM2 and p21 proteins. Compound **5** is more potent than **7**, and both compounds are more potent than racemic nutlin-3, the first bona fide potent MDM2 inhibitor reported by Vassilev and colleagues.<sup>8</sup> The levels of p53 activation by **5** at 0.5  $\mu$ M are similar to those observed by **7** at 2.5  $\mu$ M and by 10  $\mu$ M racemic nutlin-3. In contrast, MI-61 at 10  $\mu$ M, a previously reported

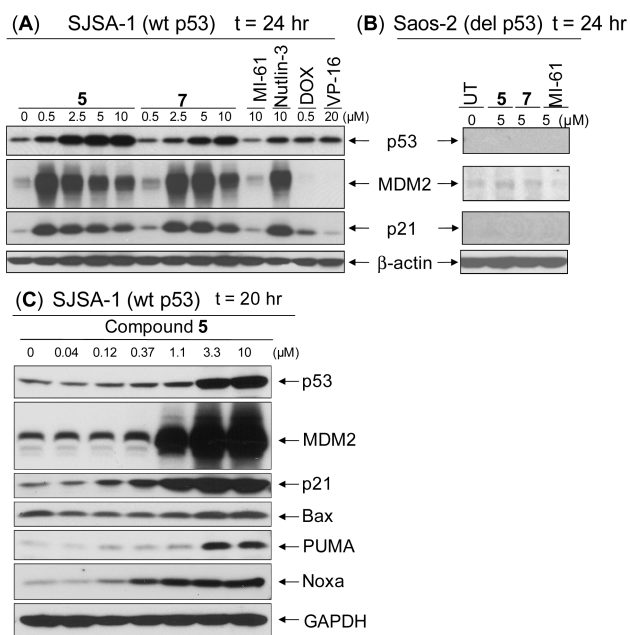


**Figure 3.** Western blot analysis of p53 activation induced by **5** and **7**. MI-61 was used as an inactive control, whereas racemic nutlin-3 was used as a positive control.

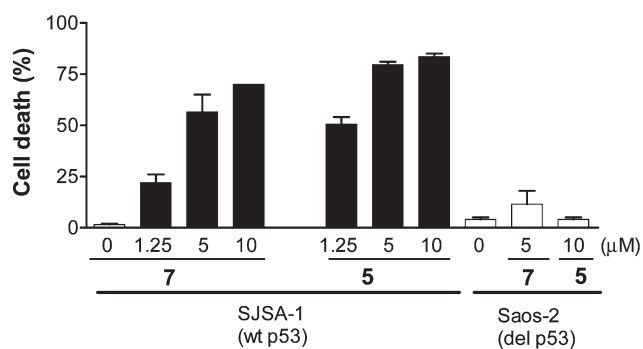


**Figure 4.** Induction of cell death by **5** and **7** in the SJSA-1 cancer cell line with wild-type p53 status and in the aOS-2 cancer cell line with deleted p53.

inactive control of compound **7**,<sup>11</sup> has little effect in induction of an accumulation of p53, MDM2, and p21 compared to untreated control, indicating the specific effect by **5** and **7**. Compounds **5** and **7** fail to induce MDM2 and p21 in the Saos-2 cell line with deleted p53 (Figure 3B), consistent with their mechanism of action as potent and specific inhibitors of the MDM2–p53 interaction (Figure 3B).<sup>8,11</sup> Compound **5** also effectively induces an increase of Bax, Puma, and Noxa in the SJSA-1 cancer cells, which are three other p53-targeted gene products and are all proapoptotic Bcl-2 members, in a dose-dependent manner (Figure 3C). A robust increase of Noxa and Puma proteins is observed with 0.37 and 3.3 μM of **5**, respectively (Figure 3C).

Activation of p53 by potent and cell-permeable MDM2 inhibitors can effectively induce tumor cells to undergo cell death.<sup>8,11</sup> Indeed, **5** and **7** are capable of inducing cell death in the SJSA-1 cell line with wild-type p53 in a dose-dependent manner (Figure 4). Compound **5** is more potent than **7**, consistent with their potencies in cell growth inhibition and in induction of p53 activation. Compound **5** at 1.25 μM is able to induce 50% of cells to undergo cell death in the SJSA-1 cell line for 2-day treatment, whereas **7** only induces 20% of cell

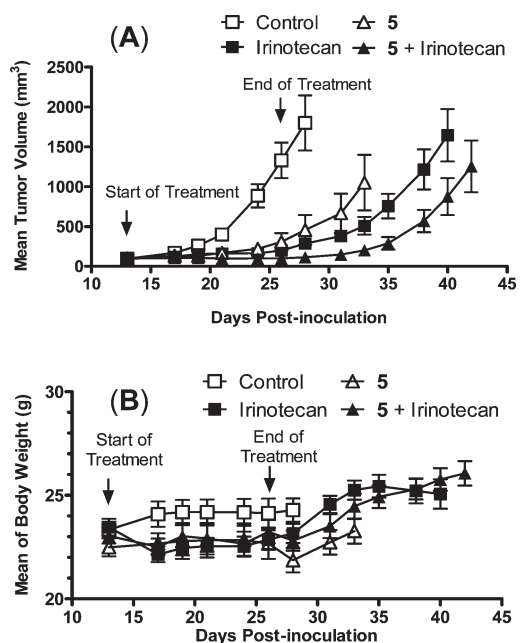


**Figure 5.** Antitumor activity of **5** alone and in combination with irinotecan in the SJSA-1 xenograft model: (A) tumor volume; (B) animal weight.

death at the same concentration. The cell death induction is specific and p53-dependent, since both compounds at 10 μM have minimal effect on the cell viability in the Saos-2 cell line with deleted p53 (Figure 4). The effective cell-death induction by **5** is also consistent with its ability to up-regulate Puma and Noxa, two potent proapoptotic proteins.

To further test the therapeutic potential for **5**, we evaluated its ability to inhibit tumor growth in the SJSA-1 xenograft model (Figure 5). Compound **5** is highly effective in inhibition of tumor growth as an oral agent. At the end of the treatment (day 26), tumors treated with the vehicle control grew to a mean volume of 1328 mm<sup>3</sup> from 95 ± 21 mm<sup>3</sup> at the start of the treatment (day 13). In comparison, tumors treated with daily, oral dose of **5** at 300 mg/kg for 14 days only grew to 308 ± 283 mm<sup>3</sup> at the end of the treatment from 100 ± 33 mm<sup>3</sup>. The *T/C* (treatment/control) for **5** is 19% when the mean tumor volume in the control group reached 750 mm<sup>3</sup> (Supporting Information). Irinotecan at a weekly 100 mg/kg intraperitoneal dose for 2 weeks, a near maximum tolerated dose, also achieved significant tumor growth inhibition and a *T/C* of 20.5% when the mean tumor volume in the control group reached 750 mm<sup>3</sup> (Supporting Information). The combination of **5** and irinotecan is statistically more effective than either agent alone (Supporting Information). The combination is able to completely inhibit tumor growth during treatment; the mean tumor volume at the end of treatment is 98 ± 47 mm<sup>3</sup>, which is the same as that at the start of the treatment (97 ± 29 mm<sup>3</sup>). There is no significant weight loss in animals treated with **5** alone and in combination with irinotecan, compared to those in the vehicle control group (Figure 5B). There are no other signs of toxicity in animals treated with **5** throughout the experiment.

The synthesis of these new compounds is similar to that reported for **1**,<sup>10</sup> and the details are provided in the Supporting Information.

We have previously performed extensive biological and pharmacological studies for **7**.<sup>11</sup> Our data demonstrated that **7** activates the p53 function in tumor cells with wild-type p53

by blocking the MDM2–p53 protein–protein interaction. While **7** also activates p53 in normal cells, it selectively induces tumor cells with wild-type p53 to undergo cell death and apoptosis but not in normal cells. In vivo, **7** induces p53 activation in xenograft tumor tissues with wild-type p53. While **7** also induces p53 activation in normal mouse tissues, it is selectively toxic to tumor tissues but not to normal mouse tissues, even after a total of 28 doses. In contrast, irinotecan and irradiation are toxic to certain normal mouse tissues. Collectively, our current and previous studies have provided strong evidence that reactivation of p53 using small-molecule inhibitors is a promising new cancer therapeutic strategy.

Although targeting protein–protein interaction using non-peptidic, small molecules has proven to be a very challenging task in modern drug discovery and medicinal chemistry, our present study has provided solid proof that it is feasible to design potent, cell-permeable, and orally active small-molecule inhibitors of the MDM2–p53 interaction. Compound **5** is arguably the most potent, specific, cell-permeable, and orally active small-molecule inhibitor discovered to date and represents a promising lead compound for further evaluation as a new class of anticancer drug.

**Acknowledgment.** We are grateful for financial support from the National Cancer Institute, National Institutes of Health (Grants R01CA121279, P50CA06956, and P50CA097248), the University of Michigan Cancer Center (Core Grant P30CA046592), the Prostate Cancer Foundation, the Leukemia and Lymphoma Society, and Ascenta Therapeutics, Inc.

**Supporting Information Available:** Experimental section, including chemical data for **2–9**, details of the fluorescence polarization-based binding assay, cell growth and cell viability assays, Western blot analysis, and in vivo animal experiment. This material is available free of charge via the Internet at <http://pubs.acs.org>.

## References

- Levine, A. J. p53, the cellular gatekeeper for growth and division. *Cell* **1997**, *88*, 323–331.
- Vogelstein, B.; Lane, D.; Levine, A. J. Surfing the p53 network. *Nature* **2000**, *408*, 307–310.
- Vousden, K. H.; Lu, X. Live or let die: the cell's response to p53. *Nat. Rev. Cancer* **2002**, *2*, 594–604.
- Wu, X.; Bayle, J. H.; Olson, D.; Levine, A. J. The p53-mdm-2 autoregulatory feedback loop. *Genes Dev.* **1993**, *7* (7A), 1126–1132.
- Chène, P. Inhibiting the p53–MDM2 interaction: an important target for cancer therapy. *Nat. Rev. Cancer* **2003**, *3*, 102–109.
- Kussie, P. H.; Gorina, S.; Marechal, V.; Elenbaas, B.; Moreau, J.; Levine, A. J.; Pavletich, N. P. Structure of the MDM2 oncoprotein bound to the p53 tumor suppressor transactivation domain. *Science* **1996**, *274*, 948–953.
- Garcia-Echeverria, C.; Chene, P.; Blommers, M. J. J.; Furet, P. Discovery of potent antagonists of the interaction between human double minute 2 and tumor suppressor p53. *J. Med. Chem.* **2000**, *43*, 3205–3208.
- Vassilev, L. T.; Vu, B. T.; Graves, B.; Carvajal, D.; Podlaski, F.; Filipovic, Z.; Kong, N.; Kammlott, U.; Lukacs, C.; Klein, C.; Fotouhi, N.; Liu, E. A. In vivo activation of the p53 pathway by small molecule antagonists of MDM2. *Science* **2004**, *303*, 844–848.
- Ding, K.; Lu, Y.; Nikolovska-Coleska, Z.; Qiu, S.; Ding, Y.; Gao, W.; Stuckey, J.; Roller, P. P.; Tomita, Y.; Deschamps, J. R.; Wang, S. Structure-based design of potent non-peptide MDM2 inhibitors. *J. Am. Chem. Soc.* **2005**, *127*, 10130–10131.
- Ding, K.; Lu, Y.; Nikolovska-Coleska, Z.; Wang, G.; Qiu, S.; Shangary, S.; Gao, W.; Qin, D.; Stuckey, J.; Krajewski, K.; Roller, P. P.; Wang, S. Structure-based design of spiro-oxindoles as potent, specific small-molecule inhibitors of the MDM2–p53 interaction. *J. Med. Chem.* **2006**, *49*, 3432–3435.
- Shangary, S.; Qin, D.; McEachern, D.; Liu, M.; Miller, R. S.; Qiu, S.; Nikolovska-Coleska, Z.; Ding, K.; Wang, G.; Chen, J.; Bernard, D.; Zhang, J.; Lu, Y.; Gu, Q.; Shah, R. B.; Pienta, K. J.; Ling, X.; Kang, S.; Guo, M.; Sun, Y.; Yang, D.; Wang, S. Temporal activation of p53 by a specific MDM2 inhibitor is selectively toxic to tumors and leads to complete tumor growth inhibition. *Proc. Natl. Acad. Sci. U.S.A.* **2008**, *105*, 3933–3938.
- Saddler, C.; Ouillette, P.; Kujawski, L.; Shangary, S.; Talpaz, M.; Kaminski, M.; Erba, H.; Shedden, K.; Wang, S.; Malek, S. N. Comprehensive biomarker and genomic analysis identifies p53 status as the major determinant of response to MDM2 inhibitors in chronic lymphocytic leukemia. *Blood* **2008**, *111*, 1584–1593.
- Shangary, S.; Ding, K.; Qiu, S.; Nikolovska-Coleska, Z.; Bauer, J. A.; Liu, M.; Wang, G.; Lu, Y.; McEachern, D.; Bernard, D.; Bradford, C. R.; Carey, T. E.; Wang, S. Reactivation of p53 by a specific MDM2 antagonist (MI-43) leads to p21-mediated cell cycle arrest and selective cell death in colon cancer. *Mol. Cancer Ther.* **2008**, *7*, 1533–1542.
- Grasberger, B. L.; Lu, T.; Schubert, C.; Parks, D. J.; Carver, T. E.; Koblisch, H. K.; Cummings, M. D.; LaFrance, L. V.; Milkiewicz, K. L.; Calvo, R. R.; Maguire, D.; Lattanze, J.; Franks, C. F.; Zhao, S.; Ramchandren, K.; Bylebyl, G. R.; Zhang, M.; Manthey, C. L.; Petrella, E. C.; Pantoliano, M. W.; Deckman, I. C.; Spurlino, J. C.; Maroney, A. C.; Tomczuk, B. E.; Molloy, C. J.; Bone, R. F. Discovery and cocrystal structure of benzodiazepinedione HDM2 antagonists that activate p53 in cells. *J. Med. Chem.* **2005**, *48*, 909–912.
- Lu, Y.; Nikolovska-Coleska, Z.; Fang, X.; Gao, W.; Shangary, S.; Qiu, S.; Qin, D.; Wang, S. Discovery of a nanomolar inhibitor of the human murine double minute 2 (MDM2)–p53 interaction through an integrated, virtual database screening strategy. *J. Med. Chem.* **2006**, *49*, 3759–3762.
- Galatin, P. S.; Abraham, D. J. A nonpeptidic sulfonamide inhibits the p53–mdm2 interaction and activates p53-dependent transcription in mdm2-overexpressing cells. *J. Med. Chem.* **2004**, *47*, 4163–4165.
- Bowman, A. L.; Nikolovska-Coleska, Z.; Zhong, H.; Wang, S.; Carlson, H. A. Small molecule inhibitors of the MDM2–p53 interaction discovered by ensemble-based receptor models. *J. Am. Chem. Soc.* **2007**, *129*, 12809–12814.
- Hardcastle, I. R.; Ahmed, S. U.; Atkins, H.; Farnie, G.; Golding, B. T.; Griffin, R. J.; Guyenne, S.; Hutton, C.; Källblad, P.; Kemp, S. J.; Kitching, M. S.; Newell, D. R.; Norbedo, S.; Northen, J. S.; Reid, R. J.; Saravanan, K.; Willems, H. M.; Lunec, J. Small-molecule inhibitors of the MDM2–p53 protein–protein interaction based on an isoindolinone scaffold. *J. Med. Chem.* **2006**, *49*, 6209–6221.
- Vassilev, L. T. p53 activation by small molecules: application in oncology. *J. Med. Chem.* **2005**, *48*, 4491–4499.
- Vassilev, L. T. MDM2 inhibitors for cancer therapy. *Trends Mol. Med.* **2007**, *13*, 23–31.
- Shangary, S.; Wang, S. Small-molecule inhibitors of the MDM2–p53 protein–protein interaction to reactivate p53 function: a novel approach for cancer therapy. *Annu. Rev. Pharmacol. Toxicol.* **2009**, *49*, 223–41.
- Shangary, S.; Wang, S. Targeting the MDM2–p53 interaction for cancer therapy. *Clin. Cancer Res.* **2008**, *14*, 5318–5324.